Journal of the Optical Society of Korea, Vol. 6, No. 3, September 2002, pp. 108-116

Lasing Modes of LD-Pumped Fiber Grating Lasers

Dongwook Park* and Joon Hwan Hwang

Department of Electronic Engineering, Hongik University, Seoul 121-791, KOREA

(Received April 2, 2002)

Lasing modes of laser-diode-pumped fiber grating lasers are analyzed by coupled-mode theory. First, a power series solution of the coupled-mode equations is derived under the assumption of an exponentially-decreasing longitudinal modal gain profile for a laser-diode-pumped grating section, followed by determination of the transfer matrix for such a section. Based on these results, an eigenvalue equation for oscillation is then derived and solved numerically for the lasing modes of uniform and phase-shifted fiber grating lasers. Comparisons made with the uniform-gain results indicate that, surprisingly, the lasing mode characteristics are not as significantly altered as might be expected in most cases, even for a highly nonuniform gain profile. In the case of a phase-shifted grating, the phase-shift position appears to have a much greater impact on determining the threshold gain, the modal field distribution, and the front-to-back output power ratio.

OCIS codes : 060.0060, 140.0140, 250.0250.

I. INTRODUCTION

There has been a growing interest in laser-diode (LD)-pumped fiber grating lasers in recent years due to their attractiveness for a variety of wavelength-division-multiplexing (WDM)- and fiber sensor-related applications [1,2]. In addition to possessing the inherent advantages of excellent spectral discrimination and built-in integration features, fiber grating lasers can be made compact and wavelength-tunable, and are easier to fabricate than the distributed Bragg reflector counterpart because the grating region itself is directly LD-pumped. Most of the published results on fiber grating lasers have, however, been mainly of experimental nature, dealing with the fabrication and characterization of the device [3,4]. While a few papers have dealt with certain theoretical aspects related to fiber grating lasers, such as the evolution of the pump and the signal beams and the population densities along the fiber and polarization-mode competition [5,6], there has been no published work up to now to the best of our knowledge dealing with how the nonuniform gain established by the pump beam affects the lasing (longitudinal) mode spectra and the associated field distributions at the threshold level. This provided the motivation for our research since results of such an analytical treatment, which has been lacking thus far, could lend a valuable insight into issues such as the side-mode-suppression ratio, the extent of spatial hole-burning, and the device's output efficiency, as well as provide a theoretical basis for design of a more complex form of fiber grating laser.

In the work presented here, we derive a power series solution to the coupled-mode equations for the case of an exponentially-decreasing longitudinal modal gain profile corresponding to a weakly-pumped fiber grating section. From this result, we obtain the transfer matrix of such a section for the eventual purpose of application toward analysis of phase-shifted structures. Based on these, we then determine semi-numerically the properties associated with the lasing modes of LD-pumped fiber grating lasers, both uniform and phase-shifted versions. In particular, the mode spectra, i.e., the normalized lasing frequency and the threshold gain, the associated field distribution, and the ratio of the forward-versus-backward power emissions of the modes are analyzed and compared to the corresponding uniform-gain results.

II. ANALYSIS

1. Power series solution for coupled-mode equations

Consider a fiber grating of length L with a uniform grating period and coupling strength. We begin the

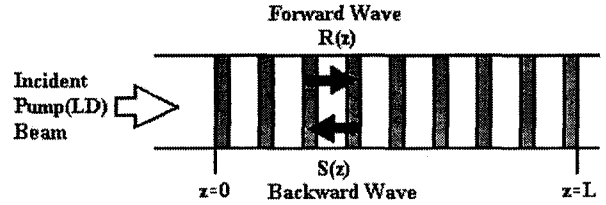

(a)

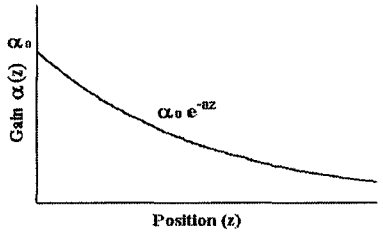

(b)

FIG. 1. Fiber grating laser model: (a) uniform fiber grating structure (b) exponentially-decreasing modal gain profile.

analysis by modifying the usual coupled-mode equations to incorporate the nonuniform gain caused by the LD pump beam incident from one side of the fiber grating laser as shown in Fig. 1(a).

$$\frac{dR(z)}{dz} = (\alpha(z) - j\delta)R(z) - j\kappa S(z) \tag{1}$$

$$\frac{dS(z)}{dz} = -(\alpha(z) - j\delta)S(z) + j\kappa^* R(z) \tag{2}$$

where $R(z)$ and $S(z)$ are the complex-amplitudes of the field components traveling in the $+z$ (forward) and $-z$ (backward) directions, respectively, δ is the frequency detuning parameter, and κ is the coupling coefficient. We take the modal gain coefficient to possess an exponentially-tapered distribution

$$\alpha(z) = \alpha_0 \exp(-\alpha z), \tag{3}$$

as shown in Fig. 1(b), given that the pump beam providing the gain is continuously absorbed as it propagates through the grating and that there is little gain saturation at the threshold.

Upon manipulating the above equations, we obtain the following pair of uncoupled equations for $R(z)$ and $S(z)$:

$$\frac{d^2}{dz^2}\begin{Bmatrix} R(z) \\ S(z) \end{Bmatrix} - \left[\pm\frac{d\alpha(z)}{dz} + (\alpha(z) - j\delta)^2 + |\kappa|^2\right]\begin{Bmatrix} R(z) \\ S(z) \end{Bmatrix} = 0 \tag{4}$$

where the upper branch (+ sign) of the $d\alpha(z)/dz$ term applies to $R(z)$ and the lower branch (− sign) to $S(z)$. This discrepancy between $R(z)$ and $S(z)$, which does not exist in the uniform-gain limit, reflects the fact that the two waves travelling in the opposite directions experience different gain variations as they propagate through the grating.

Because of the nonuniform gain, simple closed-form solutions cannot be obtained for (4). Instead, by making use of the fact that $\alpha(z)$ has a simple Taylor series expansion, we shall employ a power series representation to construct a solution for $R(z)$ and $S(z)$. We first expand $R(z)$, $S(z)$, and $\alpha(z)$ into power series of the normalized variable $u \equiv z/L$ and substitute them into (4). Then, we group the terms with the identical powers of u on the left-hand side of (4) and require the sum to be identically zero for all powers. This results in an infinite set of algebraic relations involving the unknown power series coefficients of $R(z)$ and $S(z)$. It turns out that for both $R(z)$ and $S(z)$, the corresponding power series consists of a sum of two independent parts, each part taking the form of a deterministic power series multiplied by an unknown constant. Thus, we obtain the following form of general solution for $R(z)$ and $S(z)$

$$R(u) = r_0 P_r(u) + r_1 Q_r(u) \tag{5}$$

$$S(u) = s_0 P_s(u) + s_1 Q_s(u) \tag{6}$$

where $P_r(u)$ and $Q_r(u)$, and $P_s(u)$ and $Q_s(u)$ each represent the two independent solutions (the deterministic power series functions mentioned above) of the differential equations for $R(z)$ and $S(z)$, respectively, in the presence of the exponentially-decreasing modal gain distribution. They play the role of $\cosh(\gamma z)$ and $\sinh(\gamma z)$, where $\gamma = \sqrt{|\kappa|^2 + (\alpha_0 - j\delta)^2}$, the well-known solution for $R(z)$ and $S(z)$ in the uniform gain limit $\alpha(z) = \alpha_0$. The constants γ_0, γ_1, s_0, and s_1 are the weighting factors whose relationships are to be determined from the coupled-mode equations and boundary conditions.

Following the steps described above, it can be shown that *each* of the functions $P_r(u)$, $Q_r(u)$, $P_s(u)$, and $Q_s(u)$ has a power series representation of the same generic form

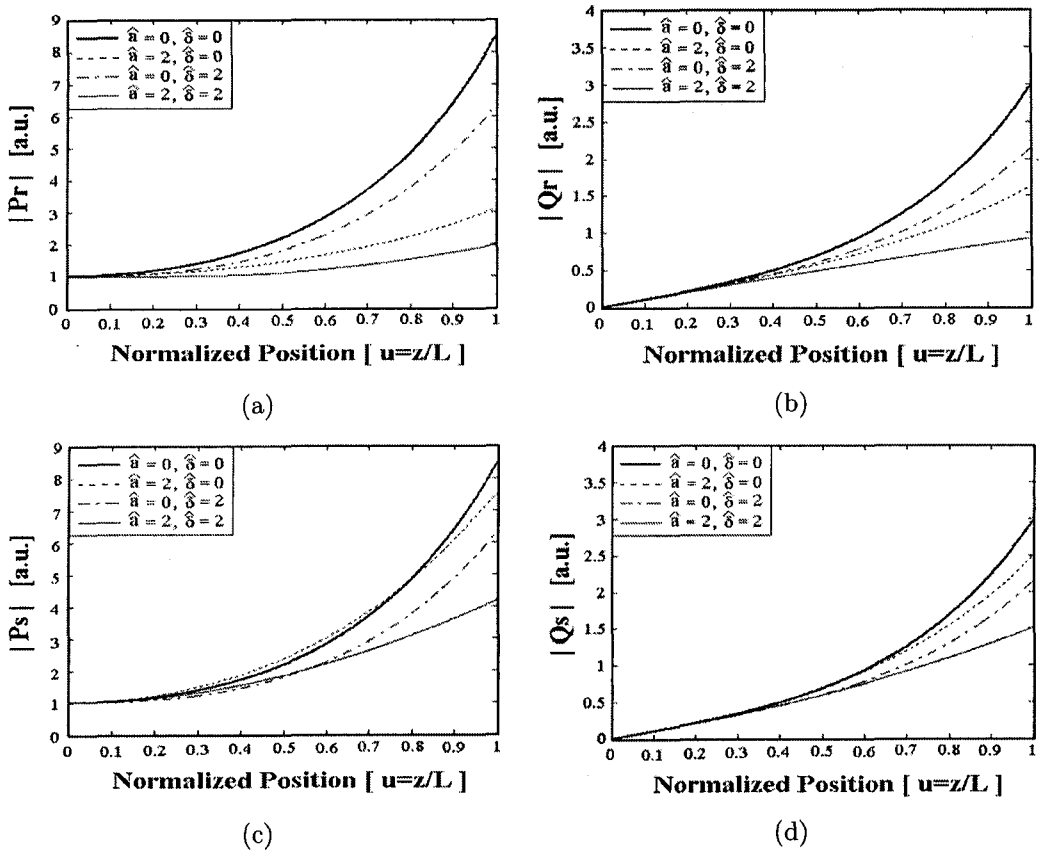

FIG. 2. Longitudinal distribution of the power series solution functions $|P_r(u)|, |Q_r(u)|, |P_s(u)|$, and $|Q_s(u)|$: (a) $|P_r(u)|$, (b) $|Q_r(u)|$, (c) $|P_s(u)|$, (d) $|Q_s(u)|$.

$$B(u) = \sum_{n=0}^{\infty} b_n u^n \tag{7}$$

The generic expression for the sets $\{p_n\}$, $\{q_n\}$, $\{p'_n\}$, and $\{q'_n\}$, $n = 0, 1, 2, \cdots$, which represent the power series coefficients for the functions $P_r(u)$, $Q_r(u)$, $P_s(u)$, and $Q_s(u)$ in (7), respectively, are given in a recursive form for $n \geq 2$ follows:

$$b_n = \frac{1}{n(n-1)} \left\{ b_{n-2}(g_0 + |\hat{\kappa}|^2 - \hat{\delta}^2) + \sum_{k=0}^{n-3} b_k g_{n-k-2} \right\} \tag{8}$$

where

$$g_m = ((-\hat{a})^m / m!)(2^m \hat{\alpha}_0^2 - \hat{\alpha}_0(2j\hat{\delta} \pm \hat{a})), \quad m \geq 0 \tag{9}$$

In the above equation, the + sign in front of $\hat{a}$ applies to $\{p_n\}$ and $\{q_n\}$ and the − sign to $\{p'_n\}$ and $\{q'_n\}$, respectively, and we have made use of parameter normalization $\hat{\alpha}_0 = \alpha_0 L$, $\hat{\delta} = \delta L$, $\hat{\kappa} = \kappa L$, and $\hat{a} = aL$. The coefficient values for the $n = 0, 1$ cases are $p_0 = p'_0 = q_1 = q'_1 = 1$ and $q_0 = q'_0 = p_1 = p'_1 = 0$, respectively.

Figs. 2 (a) - (d) display the spatial dependences of $|P_r(u)|$, $|Q_r(u)|$, $|P_s(u)|$, and $|Q_s(u)|$ for different combinations of $\hat{a}$ and $\hat{\delta}$ values, with $\hat{\kappa}$ and $\hat{\alpha}_0$ fixed at 2. $\hat{a} = 0$ and $\hat{\delta} = 0$ correspond to the uniform-gain and the Bragg wavelength conditions, respectively, and serve as a reference to illustrate how the longitudinal gain attenuation ($\hat{a} \neq 0$) and frequency detuning ($\hat{\delta} \neq 0$) affect the field distribution. Note that there are significant discrepancies between the uniform-gain and nonuniform-gain results in all the figures. In particular, $|P_r(u)|$ and $|Q_r(u)|$ distributions are different from those of $|P_s(u)|$ and $|Q_s(u)|$ when $\hat{a} \neq 0$ as a direct consequence of the sign difference in (4) and (9). These distributions, however, become identical in the limit of $\hat{a} \to 0$ as evident from the figures; in fact, $\{P_r(u), P_s(u)\}$ and $\{Q_r(u), Q_s(u)\}$ reduce to the uniform-gain solutions $\cosh(\gamma z)$ and $\sinh(\gamma z)$, respectively.

2. Transfer matrix

For analysis of fiber grating lasers consisting of complicated structures, such as phase-shifted and multi-

section gratings, transfer matrix formalism provides a convenient means of relating the input and output fields, and in fact it has been widely used for analysis of grating structures with a uniform gain and/or loss [7]. We can utilize the transfer matrix approach exactly in the same manner even in the presence of a nonuniform gain, as is the case here, provided the nonuniform nature of the gain is taken into account in deriving the transfer matrix. The grating to be analyzed, regardless of its complexity, could be divided into a number of piecewise-uniform sections, whence the transfer matrix for each section is computed in the manner described below. These transfer matrices would then be multiplied together to yield the transfer matrix for the overall structure, from which its lasing modes could be determined. A composite structure consisting of uniform sections with different grating duty cycles (but with the same grating period) could be treated similarly if the coupling coefficient value consistent with the prescribed duty cycle - to be computed by Fourier analysis of the longitudinal index profile of the grating's core - is used for each uniform section. Should the grating period vary from one section to the next as well, we also need to adjust the value of the frequency detuning parameter δ for each section - even for a fixed wavelength - as the definition of δ involves the grating period (see [8] for a discussion on limitation of the usual two-mode coupled-mode model involving such a case).

To derive the transfer matrix for a uniform grating section, i.e., a grating with constant coupling strength κ, with the presumed exponential gain profile, we first express the forward- and backward-traveling field components at the normalized location u by

$$E^+(u) = R(u)e^{-j\hat{\beta}_0 u} \tag{10}$$

$$E^-(u) = S(u)e^{+j\hat{\beta}_0 u}, \tag{11}$$

respectively, where $\hat{\beta}_0$ represents the propagation constant at Bragg wavelength normalized by length L. Evaluating them at $u = 0$ with help of (5) and (6) immediately yields the relationships

$$E^+(0) = R(0) = r_0 \tag{12}$$

$$E^-(0) = S(0) = s_0, \tag{13}$$

which relate the constants r_0 and s_0 to the (presumably known) input field components $E^+(0)$ and $E^-(0)$, respectively. In deriving (12) and (13), we have made use of the fact that $Q_r(0) = Q_s(0) = 0$ and $P_r(0) = P_s(0) = 1$. Thus, we can now express $R(u)$ and $S(u)$ in terms of $E^+(0)$, $E^-(0)$ and the unknown constants r_1, s_1. Next, these $R(u)$ and $S(u)$ expressions are substituted into the (normalized version of) coupled-mode equations (1) and (2), which produce two *linear* relations for r_1 and s_1 in terms of $E^+(0)$ and $E^-(0)$. By solving for $r_1$and s_1 in terms of $E^+(0)$ and $E^-(0)$, we can now express all four constants r_0, r_1, s_0, and s_1, and thus $E^+(u)$ and $E^-(u)$ at an arbitrary location u in terms of $E^+(0)$ and $E^-(0)$.

Based on the procedure summarized above, we can obtain the following matrix relationship between the input and the output field components:

$$\begin{bmatrix} E^+(u) \\ E^-(u) \end{bmatrix} = \begin{bmatrix} e^{-j\hat{\beta}_0 u} & 0 \\ 0 & e^{+j\hat{\beta}_0 u} \end{bmatrix} \begin{bmatrix} P_r(u) + AQ_r(u) & BQ_r(u) \\ CQ_s(u) & P_s(u) + DQ_s(u) \end{bmatrix} \begin{bmatrix} E^+(0) \\ E^-(0) \end{bmatrix} \tag{14}$$

where

$$A = \frac{1}{\triangle}\left[\ |\hat{\kappa}|^2 P_r(u)Q_s(u) - \{P_r'(u) - MP_r(u)\}\{Q_s'(u) + MQ_s(u)\}\ \right] \tag{15}$$

$$B = \frac{1}{\triangle}\left[\ \hat{\kappa}P_s(u)\{Q_s'(u) + MQ_s(u)\} - \hat{\kappa}Q_s(u)\{P_s'(u) + MP_s(u)\}\ \right] \tag{16}$$

$$C = \frac{1}{\triangle}\left[\ \hat{\kappa}^* P_r(u)\{Q_r'(u) - MQ_r(u)\} - \hat{\kappa}^* Q_r(u)\{P_r'(u) - MP_r(u)\}\ \right] \tag{17}$$

$$D = \frac{1}{\triangle}\left[\ |\hat{\kappa}|^2 Q_r(u)P_s(u) - \{P_s'(u) + MP_s(u)\}\{Q_r'(u) - MQ_r(u)\}\ \right] \tag{18}$$

$$\triangle = \{Q_r'(u) - MQ_r(u)\}\{Q_s'(u) + MQ_s(u)\} - |\hat{\kappa}|^2 Q_s(u)Q_r(u) \tag{19}$$

$$M = \hat{\alpha}_0 e^{-\hat{a}u} - j\hat{\delta} \tag{20}$$

In the above, a prime ($'$) denotes a derivative with respect to u. Of course, this result reduces to that of the standard transfer matrix in the uniform-gain case as $\hat{a} \to 0$, i.e., as the gain's nonuniformity disappears.

3. Lasing modes

Next we shall derive an eigenvalue equation for the lasing condition that would allow us to determine the oscillation frequency and the required gain of the lasing modes *at threshold*, and also analyze their end-emission characteristics. We shall first examine the case of a laser composed of a single uniform fiber grating section, and then proceed to the more complicated case of a laser utilizing a phase-shifted fiber grating section. In both cases, the boundary condition of zero reflection at two ends of the grating structure imposes the following requirement of

$$R(u=0) = S(u=1) = 0 \tag{21}$$

This zero-reflection boundary condition at both ends is based on the assumption that the fiber grating is part of a fiber segment and not detached from it.

A. Uniform fiber grating laser

Upon applying the boundary condition (21) and by making use of the coupled-mode relations (1) and (2) at $u = 0$ ($z = 0$) and also the fact that $Q_r(0) = Q_s(0) = P_r'(0) = P_s'(0) = 0$, $Q_r'(0) = Q_s'(0) = 1$, we can obtain the following expressions for the $R(z)$ and $S(z)$ distributions within the uniform grating fiber laser:

$$R(u) = Q_r(u) \tag{22}$$

$$S(u) = \frac{j}{\hat{\kappa}}\left(P_s(u) - \frac{P_s(1)}{Q_s(1)}Q_s(u)\right) \tag{23}$$

In the above equations, the amplitude scaling factor has been set to unity for convenience since we are performing only a linear analysis in this paper. Upon comparing (22) and (23) with the general solution as given by (5) and (6), we note that the constants r_0, r_1, s_0, and s_1 appearing in (5) and (6) take on the values of 0, 1, $j/\hat{\kappa}$, and $-jP_s(1)/\hat{\kappa}Q_s(1)$, respectively,

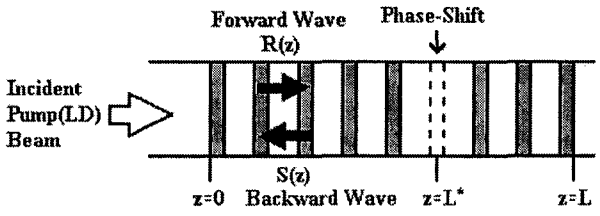

FIG. 3. Phase-shifted fiber grating laser model.

in this case. Applying the coupled-mode relations once again, this time at $u = 1$ ($z = L$), yields the desired eigenvalue equation

$$Q_r'(1)/Q_r(1) = \hat{\alpha}_0 e^{-\hat{a}} - j\hat{\delta} \tag{24}$$

The set of $(\hat{\delta}, \hat{\alpha}_0)$ values satisfying (24) for the given $\hat{\kappa}$ and $\hat{a}$ values correspond to the normalized (detuned) frequency and the threshold modal gain of the lasing modes for the uniform fiber grating laser.

B. Phase-shifted fiber grating laser

When the fiber grating laser is based on a phase-shifted structure, i.e., with a phase-shift in the grating profile at some location, the field distribution on the two sides of the phase-shift takes on a distinctively different appearance and thus cannot be uniformly represented by the same set of functions. As a result, the lasing condition cannot be cast in a simple equation form such as (24) in this case. Instead, it is more convenient to make use of the transfer matrix introduced earlier to obtain the corresponding eigenvalue equation as shown below.

Assume that the grating phase-shift is located at $z = L^*$ (see Fig. 3). Then, we can relate the forward- and backward-traveling electric field components at the left facet ($z = 0$) to those at the right facet ($z = L$) as follows:

$$\begin{bmatrix} E^+(L) \\ E^-(L) \end{bmatrix} = \left[T^{(2)}\right]\left[T^{(1)}\right]\begin{bmatrix} E^+(0) \\ E^-(0) \end{bmatrix} = [T]\begin{bmatrix} E^+(0) \\ E^-(0) \end{bmatrix} \tag{25}$$

where

$$\left[T^{(i)}\right] = \begin{bmatrix} t_{11}^{(i)} & t_{12}^{(i)} \\ t_{21}^{(i)} & t_{22}^{(i)} \end{bmatrix} = \begin{bmatrix} e^{-j\hat{\beta}_0 u_i} & 0 \\ 0 & e^{+j\hat{\beta}_0 u_i} \end{bmatrix}\begin{bmatrix} P_r(u_i) + A_i Q_r(u_i) & B_i Q_r(u_i) \\ C_i Q_s(u_i) & P_s(u_i) + D_i Q_s(u_i) \end{bmatrix}, \quad i = 1, 2 \tag{26}$$

In the above, $[T^{(1)}]$ and $[T^{(2)}]$ are the transfer matrices for the section to the left of the phase-shift, i.e., for $0 \leq z \leq L^*$, and for the section to the right, i.e., for $L^* \leq z \leq L$, respectively, and u_1 and u_2 are the normalized lengths of the two sections, L^*/L and $(L - L^*)/L$. Thus, $[T]$, the product of the two matrices, represents the transfer matrix for the total phase-shifted grating structure. Although the same functional form of (15)-(20) applies in evaluating both $[T^{(1)}]$ and $[T^{(2)}]$, $\hat{\alpha}_0$ must be replaced by $\hat{\alpha}_0 e^{-au_1}$, the normalized gain at the beginning of the section to the right, for the latter, assuming that the exponential taper of the modal gain is unaffected by the phase-shift. Similarly, the value of $\hat{\kappa}$ to be used in evaluation of $[T^{(2)}]$ must be adjusted by taking into account the correct grating phase at $z = L^{*+}$.

To determine the eigenvalue equation for lasing condition, we impose the condition $E^+(0) = E^-(L) = 0$ on (25) to be consistent with the self-oscillating nature of lasing and the zero end-reflection assumption

$$\begin{bmatrix} E^+(L) \\ 0 \end{bmatrix} = [T] \begin{bmatrix} 0 \\ E^-(0) \end{bmatrix} = \begin{bmatrix} t_{11} & t_{12} \\ t_{21} & t_{22} \end{bmatrix} \begin{bmatrix} 0 \\ E^-(0) \end{bmatrix} \tag{27}$$

from which we obtain the desired eigenvalue equation of the phase-shifted fiber grating laser as follows:

$$t_{22} = t_{21}^{(2)} t_{12}^{(1)} + t_{22}^{(2)} t_{22}^{(1)} = 0 \quad \Rightarrow \quad \frac{t_{21}^{(2)}}{t_{22}^{(2)}} = -\frac{t_{22}^{(1)}}{t_{12}^{(1)}} \tag{28}$$

As with the earlier case, the set of $(\hat{\delta}, \hat{\alpha}_0)$ values satisfying the eigenvalue equation, (28) this time, constitute the lasing modes of the phase-shifted grating laser.

III. NUMERICAL RESULTS AND DISCUSSION

In this section, numerical results pertaining to the mode spectrum, the mode field distribution, and the associated side (end)-emission ratio will be presented and discussed for the two types of lasers analyzed above. With the uniform grating laser, the following three cases were examined that correspond to different levels of erbium and/or ytterbium doping density: (a) $\hat{a} = 0$ (uniform gain); (b) $\hat{a} = 0.5$; and (c) $\hat{a} = 1$. Cases (b) and (c) correspond to attenuation of the power gain at the grating's right end by a factor of $e^{-1} \approx 0.37$ and $e^{-2} \approx 0.14$, respectively, relative to that at the left end. As for the phase-shifted grating laser, six different cases were analyzed with various combinations of the phase-shift position ($z = 0.25L, 0.5L$, and $0.75L$) and the $\hat{a}$ value ($\hat{a} = 0, 2$), all with the grating phase-shift of π, corresponding to the quarter-wavelength phase-shifted

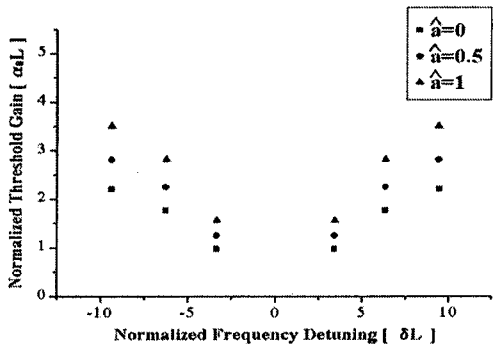

(a)

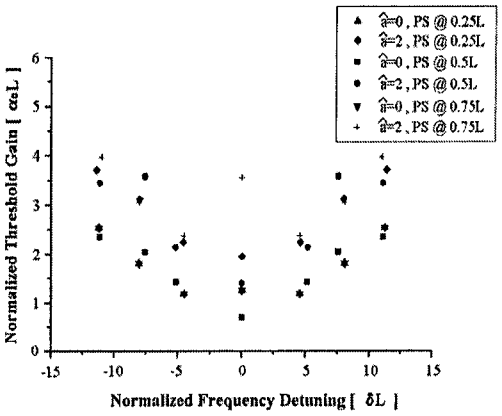

(b)

FIG. 4. Lasing mode spectrum: (a) uniform grating laser (b) phase-shifted grating laser.

(QWPS) case. Although the phase-shift locations of $z = 0.25L$ and $z = 0.75L$ are symmetric with respect to the center of the structure, both cases were included nonetheless to examine the effects of the asymmetric modal gain distribution caused by the nonuniform pumping, i.e., pumping from only one particular side. In all calculations, the $\hat{\kappa}$ value was held constant at 2, and typically no more than 30-40 terms were required for convergence of the power series for $P_r(u), Q_r(u), P_s(u)$, and $Q_s(u)$.

The lasing mode spectrum can reveal useful information regarding the laser's threshold gain and the side-mode-suppression ratio. Figs. 4(a) and (b) show the computed mode spectra for the uniform (zero phase-shift) and the phase-shifted fiber grating lasers, respectively. We note from Fig. 4(a) that the mode spectrum for each uniform grating case is symmetric with respect to $\hat{\delta} = 0$, i.e., the Bragg wavelength, even in the presence of a nonuniform gain, giving rise to a doubly-degenerate mode spectrum structure. This feature, whose generality can easily be proved, is similar to that of a purely index-coupled uniform-gain semiconductor distributed-feedback (DFB) laser.

Surprisingly, the general features of the mode spectra for the nonuniform-gain cases ($\hat{a} \neq 0$) are not significantly different from those of the uniform-gain case ($\hat{a} = 0$). The normalized mode frequencies are nearly the same as before and although there are definite increases in the threshold gain due to the lower average gain across the grating length compared to the uniform-gain case, the differences are not dramatic, especially for the lower-order modes.

Most of the above remarks apply to the phase-shifted grating laser results in Fig. 4(b) as well, with the exception of the additional nondegenerate mode's appearance at $\hat{\delta} = 0$, which is also consistent with the previous findings regarding the index-coupled, uniform-gain QWPS DFB laser. However, there are other aspects of Fig. 4(b) that are worth mentioning. The foremost is that the location of the phase-shift has a strong influence on the mode spectrum, especially in the presence of a nonuniform gain. The uniform-gain results for the three different phase-shift positions are closely bunched, with the lowest-order mode (fundamental mode) for the centered ($z = 0.5L$) case possessing the minimum threshold gain value. While the corresponding nonuniform-gain results are generally closely grouped together as well, there are two major differences between the two sets of results. For one, the modes for the nonuniform-gain cases have substantially higher threshold gain values. Moreover, because a higher gain attenuation rate ($\hat{a} = 2$) was assumed for the phase-shifted grating calculations - as opposed to $\hat{a} = 0.5$ and $\hat{a} = 1$ for the uniform grating calculations - the extent of increase in the threshold gain over the corresponding uniform-gain results is larger overall than in the uniform grating results. The other major difference is that the degeneracy between the $z = 0.25L$ and $z = 0.75L$ cases which had existed in the uniform-gain regime is now broken. To wit, the mode spectra of the two cases are identical in the uniform-gain regime - as evidenced by the complete overlap of the two results (marked by upright and inverted triangles) in Fig. 4(b) - but they are separated in the nonuniform-gain regime (denoted this time by diamond and cross symbols, respectively), with the lowest-order mode for the $z = 0.75L$ case now possessing a very large threshold gain.

A physical explanation for the aforementioned dis-

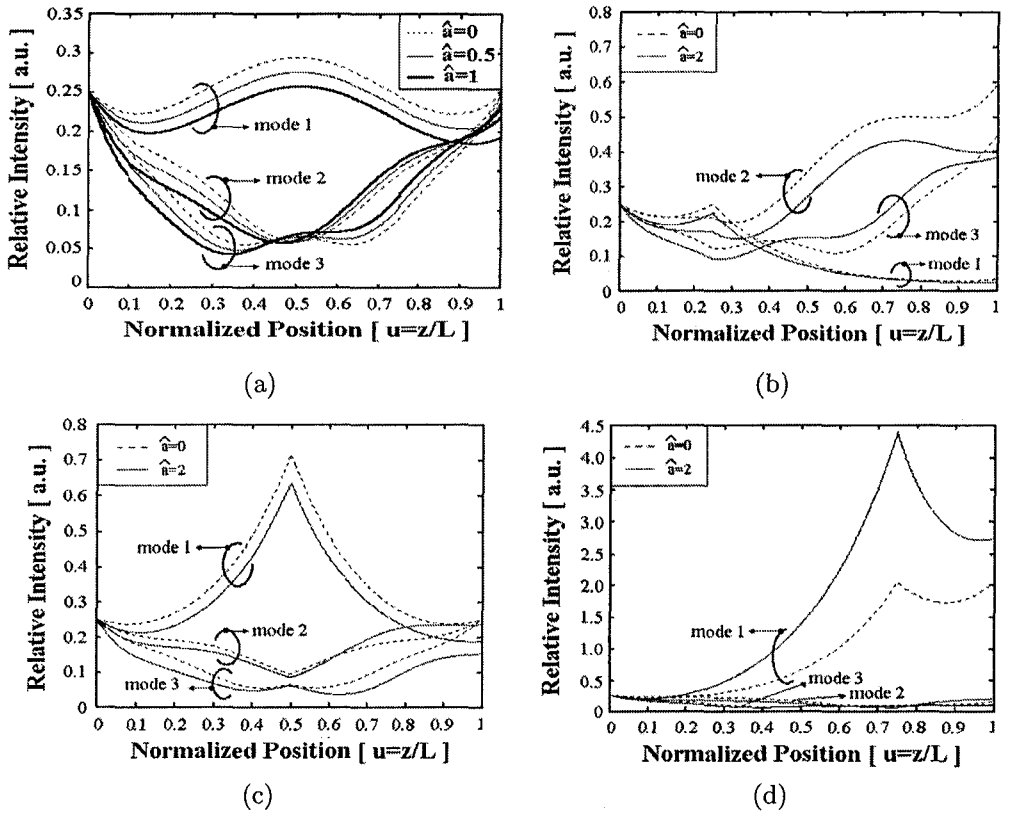

FIG. 5. Relative intensity distribution $|R(u)|^2 + |S(u)|^2$ for the three lowest-order modes: (a) uniform grating laser (b) phase-shifted grating laser with the phase-shift at $z = 0.25L$ (c) phase-shifted grating laser with the phase-shift at $z = 0.5L$ (d) phase-shifted grating laser with the phase-shift at $z = 0.75L$.

TABLE 1. Forward-to-backward output intensity ratio: (a) uniform grating laser (b) phase-shifted grating laser (L^* : phase-shift location).

	$\hat{a}=0$	$\hat{a}=0.5$	$\hat{a}=1$
Mode 1	1.000	0.879	0.773
Mode 2	1.000	0.936	0.877
Mode 3	1.000	0.960	0.922

(*a*)

	$\hat{a}=0$ $L^*=0.25L$	$\hat{a}=0$ $L^*=0.5L$	$\hat{a}=0$ $L^*=0.75L$	$\hat{a}=2$ $L^*=0.25L$	$\hat{a}=2$ $L^*=0.5L$	$\hat{a}=2$ $L^*=0.75L$
Mode 1	0.123	1.000	8.112	0.086	0.751	10.87
Mode 2	2.364	1.000	0.423	1.611	0.939	0.340
Mode 3	1.786	1.000	0.560	1.530	0.611	0.742

(*b*)

crepancy can be given as follows. With a uniform gain, the two cases with the phase-shift at $z = 0.25L$ and $z = 0.75L$ represent structures - gain profile included - that are mirror images of each other and thus they must possess identical mode properties. However, once this structural symmetry is broken by the nonuniform gain profile due to LD-pumping from the $z = 0$ side, the two cases represent physically different structures and consequently the lasing modes become distinguishable. The fact that the lowest-order mode's threshold gain for the $\hat{a} = 2$, $z = 0.75L$ case is so much greater is one direct consequence of such bifurcation. Specifically, because the field gain is diminished to a much lower level - by a factor of $e^{-\hat{a}u} = e^{-(2)(0.75)} \approx 0.22$ relative to the initial gain α_0 - at the phase-shift location $z = 0.75L$, around which the field energy associated with the lowest-order mode at $\hat{\delta} = 0$ is highly concentrated (see "mode 1" in Fig. 5(d)), we would expect that the gain attenuation would have a much more adverse impact on this particular mode compared to the other modes that possess a more even distribution.

The modal field distribution provides important information regarding the extent of spatial hole-burning and the side-emission ratio that can be expected when the laser is lasing in that particular mode. Figs. 5 (a)-(d) represent the combined intensity distribution $|R(u)|^2 + |S(u)|^2$ on a normalized scale for the three lowest-order modes associated with the uniform grating (Fig. 5 (a)) and the QWPS grating results (Figs. 5 (b)-(d) for the phase-shift locations of $z = 0.25L$, $0.5L$, and $0.75L$, respectively) discussed above. Since the degenerate modes at (δ, α_0) and $(-\delta, \alpha_0)$ possess the same intensity distribution, only the modes in the $\delta \geq 0$ region are shown here, with the mode number assigned according to its proximity to the Bragg wavelength ($\hat{\delta} = 0$). The most obvious feature seen from these figures is that in all nonuniform-gain results, deviations from the corresponding uniform-gain results are evident in the form of their asymmetric distributions - with respect to the center of the grating $u = 1/2$ - and the greater undulation of these distributions. Generally speaking, the extent of these undulations becomes more pronounced with the increasing $\hat{a}$ value (gain nonuniformity) and the mode order. However, as with the mode spectrum results earlier, the deviations between the uniform-gain and the nonuniform-gain results are not for the most part as noticeable as one might expect, given the magnitude of the gain nonuniformities. We believe that this is probably due to the grating-assisted coupling between the forward and backward waves: evidently, impact of the asymmetry in the gain profile as "seen" by the two waves is greatly tempered by the continuous exchange of power between them. Without this distributed-feedback mechanism, for example as in a fiber laser constructed from a plain uniform fiber section with cleaved ends, gain nonuniformity due to side-pumping should lead to more profound changes.

An exception to the rule is the lowest-order mode (mode 1) of the QWPS case with the phase-shift at $z = 0.75L$. Unlike the other modes, its energy is concentrated primarily near the phase-shift location where the gain attenuation happens to be quite appreciable. As a result, this mode undergoes the most dramatic change in reference to the uniform-gain result, as borne out by the sharp increase in its threshold gain (see Fig. 4(b)) and the significant increase in its relative intensity in the neighborhood of the phase-shift location (see Fig. 5(d)).

Another useful piece of information that can be gleaned from the modal distribution is the side-emission ratio, i.e., the ratio of the forward and backward output intensities, $X \equiv |R(1)/S(0)|^2$. From a practical standpoint, we would like a laser to emit most of its power to just one side, corresponding to either $X \gg 1$ or $X \ll 1$. For the purpose of comparison, the side-emission ratio of the three lowest-

order modes was tabulated in Table 1 (a) and (b) for each of the cases mentioned above. The results can be summarized as follows. First, the side-emission ratio for the uniform grating and the centered-QWPS grating (the phase-shift at $z = 0.5L$) is unity in the uniform-gain limit regardless of the mode because of their symmetric structures. However, the ratio diminishes to lower values in the presence of gain nonuniformity, implying more emission in the backward direction, since the symmetry is now broken. The fact that the forward emission is less than the backward emission in these cases is a manifestation of the forward wave being influenced more by the exponential tapering of the longitudinal gain distribution. Second, the emission ratios are the inverses of each other in the uniform-gain limit for the QWPS cases with the phase-shift at $z = 0.25L$ and $z = 0.75L$, respectively, as the two structures are mirror images of each other in this situation. In particular, the emission on the side nearer to the phase-shift location is greater than the emission on the opposite side by a factor of 8 or so for the fundamental mode. In the presence of gain attenuation, this inverse relation between the two sets of emission ratios is no longer preserved, with the ratio of the stronger emission over the weaker emission for the fundamental mode of the both cases now approaching the neighborhood of 11. Thus, looking at just the emission ratio, the fundamental mode of the grating laser with the phase-shift located towards one end of the structure is seen to produce a highly directional output, with the directionality actually being enhanced by nonuniform-gain. By comparison, the emission ratios of other modes are only in the range of 0.340 to 2.364.

In this section, we have examined the threshold gain, intensity distribution and the side-emission ratio associated with the lasing modes of LD-pumped uniform grating and phase-shifted (QWPS) grating structures under a variety of conditions. Based on these results, we conclude that the impact a nonuniform gain profile has on the modal properties is less severe than expected, except for the fundamental mode when the phase-shift location is near the far-end of the structure. As far as the "optimum" case/mode is concerned, while the fundamental mode of the centered phase-shift case possesses the minimum threshold gain with or without gain nonuniformity, the fundamental mode associated with the phase-shift location at $z = 0.25L$ possesses the most desirable side-emission ratio, i.e., directional property, at a reasonable threshold gain among the cases analyzed. The only drawback of this mode is that most of its output power is emitted at the near-end where the pump beam is injected, which could make output coupling somewhat cumbersome.

IV. CONCLUSION

We obtained the longitudinal mode characteristics of LD-pumped fiber grating laser at threshold by using a power series solution based on the assumption of an exponentially-decreasing gain distribution. The mode features, for the most part, were found to be surprisingly similar to those of the uniform-gain results even for a highly nonuniform gain distribution. For phase-shifted fiber grating lasers, the phase-shift location appears to play a more important role than the gain attenuation itself in determining the side-emission ratio and the threshold gain. However, the gain attenuation does break the structural symmetry and as a result phase-shift location near the LD-pumped end is deemed more preferable than at the opposite end. The power series solution to the coupled-mode equations and the corresponding transfer matrix derived here should also be applicable to a similar threshold analysis of LD-pumped fiber grating structures of arbitrary complexity.

ACKNOWLEDGEMENT

This research was supported in part by the Hongik University Academic Research Support Fund for the year 2000.

*Corresponding author : dwpark@wow.hongik.ac.kr

REFERENCES

[1] J.-L. Archambault and S. G. Grubb, J. Lightwave Technol. **15**, 1378 (1997).
[2] W.-C. Du, X.-M. Tao, and H.-Y. Tam, IEEE Photon. Technol. Lett. **11**, 105 (1999).
[3] W. H. Loh, B. N. Samson, L. Dong, G. J. Cowle, and K. Hsu, J. Lightwave Technol. **16**, 114 (1998).
[4] W. H. Loh and R. I. Laming, Electron. Lett. **31**, 1440 (1995).
[5] F. DiPasquale, IEEE J. Quantum Electron. **32**, 326 (1996).
[6] E. Ronnekleiv, M. N. Zervas, and J. T. Kringlebotn, IEEE J. Quantum Electron. **34**, 1559 (1998).
[7] H. Ghafouri-Shiraz and B. S. K. Lo, *Distributed Feedback Laser Diodes: Principles and Physical Modelling* (John Wiley & Sons, Chichester, 1996) pp. 105-127.
[8] D. Park and J. H. Hwang, J. of IEEK **37SD**, 673 (2000).